Hydrophobic Polymer Melt, Tethered to the Water Surface—Monolayers of Polyisoprenes with Sulfonate Head Groups†

Robert Heger and Werner A. Goedel*

Max-Planck Institut für Kolloid- & Grenzflächenforschung, Haus 9.9, Rudower Chaussee 5, 12489 Berlin, Germany

Received June 10, 1996[⊗]

ABSTRACT: Hydrophobic polymers with low glass transition temperature (polyisoprenes) and a single head group (sulfonate) have been synthesized and characterized as insoluble monolayers on a water surface. The films are considerably thicker (10−50 nm) than conventional Langmuir monolayers of low molecular weight substances or polymers with surface-active repeating units. The thickness is inversely proportional to the area per head group. Films can be transferred via the Langmuir−Blodgett technique with transfer ratios close to 1. We use these monolayers as model systems to investigate the influence of the polymer chain statistics on the properties of solvent-free tethered polymers. We assume that each polymer chain is bound to the water phase with the head group and has the conformation of a distorted three-dimensional coil. The distortion increases with decreasing area per head group (A/n) and influences the isotherm of the polymer monolayers. We develop a theoretical description of this effect and conclude that, at a given area per head group, the surface pressure increases linearly with the chain length. In the case of Gaussian statistics, the slope of this line is proportional to the third power of the area per head group. In the case of non-Gaussian statistics, this slope can be expressed as a polynomial of A/n. The experimental data confirm these theoretical predictions. Deviations from Gaussian statistics can be neglected, and the description as a nonuniformly stretched brush (Semenov theory) comes closer to the experiment than the model of a uniformly stretched brush. Chains shorter than 300 repeat units systematically deviate from the theory.

Introduction

A "polymer brush" is composed of flexible polymers bound with one end (the head group) to a surface with a lateral spacing considerably less than the dimensions of the undisturbed polymer coil. The neighboring chains interact with each other, and the polymer forms a continuous film.

In general, we have to distinguish two cases: a solvent-free brush of a polymer melt ("melt brush" or "dense brush", see Figure 1a) and a polymer brush in contact with a good solvent ("swollen brush", see Figure 1b). In the first case, there is no solvent to fill voids between polymer segments. Therefore, the concentration of segments is essentially fixed due to the balance between strong attraction and hard-core repulsion. In the latter case, the interaction is primarily osmotic. In both cases, the interaction between neighboring chains leads to a distortion of the coils, which are forced away from the interface. The "brush" is considerably thicker than monolayers of polymers which absorb with each repeat unit.

The dense brush has its main importance in the context of phase-separated block copolymers. In these systems, incompatible polymer chains are linked together but phase separate into small domains. The link between the chains is in the interface between the domains, and these systems can be regarded as a bulk material made out of dense polymer brushes. The often complex morphologies of these systems (e.g., lamellar [see Figure 1c], hexagonal, cubic, ...) are a result of the balance between the interfacial tension and the interactions of the closely packed polymer chains, which tend to stretch and bend the interface.[1−6] The swollen brush is especially important in the context of surface modification, especially in the steric stabilization of colloids and dispersed particles.[7,8]

While there is considerable interest in these highly dispersed bulk systems, it has been very advantageous to study polymer brushes as *monolayers at flat surfaces*. In such a monolayer, it is relatively easy to determine and tune the surface concentration of the head groups and to give the system a preferred orientation in space. In addition, monolayers at liquid surfaces offer a convenient method to apply polymer layers of controlled thickness to solid substrates using the Langmuir−Blodgett technique.[9]

Most of the investigations of monolayers at flat surfaces, however, concentrate on swollen brushes,[10−18] and only a few investigations on monolayers of dense polymer brushes have been published. It has been shown that hydrophobic polymers with hydrophilic head groups, applied to a water surface, give rise to reproducible isotherms,[19] can be transferred to solid substrates,[20−22] and can be degraded to form mechanically stable inorganic coatings.[23] The molecular weights of the polymers used, however, have been comparatively low, the systems being very similar to low molecular weight substances.

Until now, no study linked the properties of these films to characteristic "polymeric" effects, such as the chain statistics. It is obvious that increasing the molecular weight of the polymers should eventually lead to a system in which the chain statistics dominate the properties. It is an open question, however, whether such systems can be realized, e.g., whether a polymer chain long enough to influence the isotherm will not cause the detachment of a small head group.

In this paper, we investigate the *effects of chain length* on the properties of *monolayers* of *dense polymer brushes*. In particular, we want to show (i) that there is a regime

* To whom correspondence should be addressed. Tel.: ++49 30 6392 3118. Fax: ++49 30 6392 3115 or ...3102. E-mail: goedel@mpikg.fta-berlin.de. http://www.mpikg-teltow.mpg.de/goedel.html.

† Dedicated to Prof. D. Woermann on the occasion of his retirement.

⊗ Abstract published in *Advance ACS Abstracts,* December 1, 1996.

S0024-9297(96)00837-6 CCC: $12.00

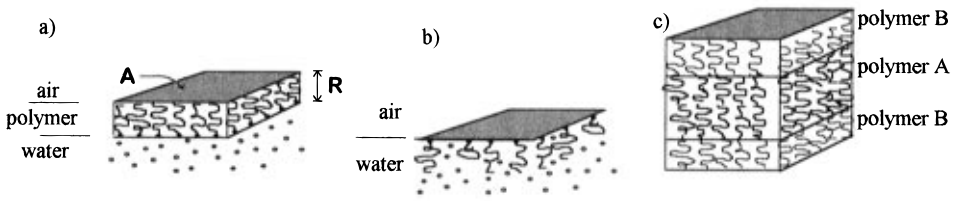

Figure 1. Schematic comparison of (a) monolayers of tethered polymers that are free of solvent, (b) monolayers of tethered polymers swollen with solvent, and (c) one lamella of phase-separated block copolymers.

of stable brushes of polymer melts in which the polymer chain statistics dominate the properties of the film, (ii) that these films can be used to generate thin and smooth polymer films of controlled thickness, and (iii) that the properties can be described quantitatively using polymer theory.

Theory

We regard the polymer as a continuous layer of uniform thickness that is free of solvent and that has one interface with the aqueous phase and one interface with the air (Figure 1a). All polymer chains are bound to the aqueous phase by one end (the head group). The system is characterized by the area of this interface, A, the temperature, T, the number of polymer chains in the system, n, and the properties of the polymer chains.

It is obvious that, at "very high" and "very low" areas per head group, the film will be energetically unstable and either break up into islands or collapse. We limit our considerations only to the regime of a stable film.

The measured film pressure is given by the difference between the derivatives of the free energy with respect to area of the pure water surface and the adsorbed polymer layer:

$$\Pi = -\left(\frac{\partial F}{\partial A}\right)_{\text{polymer film}} + \left(\frac{\partial F}{\partial A}\right)_{\text{water/air interface}} \quad (1)$$

We postulate that the first term in eq 1 can be represented by the sum of the following three contributions: (i) the interfacial tension at the polymer/air interface, (ii) the interfacial tension at the polymer/water interface, and (iii) a contribution to the surface pressure due to an elastic stretching of the polymer chains (the van der Waals interactions between air and water through the polymer film can be neglected, see Appendix A):

$$\Pi = -\left(\frac{\partial F}{\partial A}\right)_{\text{polymer/air interface}} - \left(\frac{\partial F}{\partial A}\right)_{\text{water/polymer interface}} - \left(\frac{\partial F}{\partial A}\right)_{\text{elastic}} + \left(\frac{\partial F}{\partial A}\right)_{\text{water/air interface}} \quad (2)$$

The last term of eq 2 is the surface tension of clean water:

$$\left(\frac{\partial F}{\partial A}\right)_{\text{water/air interface}} = \gamma_{\text{wa}} = \text{constant} \quad (3)$$

We assume that the free ends are similar to the other segments of the chain and do not influence the surface tension of the interfaces, even in cases when their surface concentration might be significant. Thus, the surface tension of the polymer/air interface is independent of the area per molecule.

$$\left(\frac{\partial F}{\partial A}\right)_{\text{polymer/air interface}} = \gamma_{\text{pa}} = \text{constant} \quad (4)$$

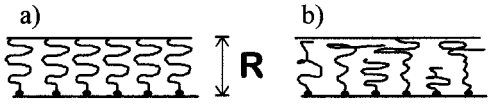

Figure 2. Schematic comparison between (a) a uniformly stretched brush and (b) a nonuniformly stretched polymer brush similar to the Semenov scenario.

The head groups of the polymer chains, however, are chemically different from the polymer chain, and the surface concentration of these groups does influence the interfacial tension of the polymer/water interface. In general, the presence of the head groups tends to lower the surface tension compared to the value, γ°_{wp}, for the polymer/water interface free of head groups. One might choose to represent this dependency using a simple two-dimensional ideal gas equation or more sophisticated theories; at this point, it is sufficient to point out the dependency in a general form. Because, in this term, we consider only interfacial phenomena and regard the adjacent polymer layer essentially as bulk material, this term does not depend on the chain length, N, of the polymer:

$$\left(\frac{\partial F}{\partial A}\right)_{\text{water/polymer interface}} = \gamma^\circ_{\text{wp}} - f\left(\frac{A}{n}, \text{ not } N\right) \quad (5)$$

If we apply eqs 3−5 on eq 2, we obtain

$$\Pi = \gamma^* + f\left(\frac{A}{n}, \text{ not } N\right) - \left(\frac{\partial F}{\partial A}\right)_{\text{elastic}} \quad (6)$$

with

$$\gamma^* = \gamma_{\text{wa}} - (\gamma_{\text{pa}} + \gamma^\circ_{\text{wp}})$$

To calculate the contribution of the elastic deformation, $(\partial F/\partial A)_{\text{elastic}}$, we consider three different systems: (a) a simple "uniformly stretched brush" of Gaussian chains, (b) the more refined self-consistent brush of Gaussian chains following the Semenov theory, and (c) a "uniformly stretched brush" of chains following the inverse Langevin approximation.

(a) Uniformly Stretched Gaussian Brush. We assume that all chains are uniformly stretched. One end is tethered to the polymer/water interface, and the other end is at the polymer/air interface (see Figure 2a).

We regard the polymer as a freely jointed chain, which is characterized by the number of polymer chains in the system, n, the number of segments of each chain, N_{f}, the volume of each segment, v_{f}, and the flexibility of the chain, which is given by either the effective radius of gyration of a segment, a_{f}, the statistical segment length, l_{f}, or the undisturbed mean square end-to-end distance, $\langle r^2\rangle_0 = 6a_{\text{f}}^2 N_{\text{f}} = l_{\text{f}}^2 N_{\text{f}}$. (In the following, the subscript f indicates the freely jointed chain.)

In the Gaussian approximation, the change in entropy upon separating both ends by the film thickness, R, is[24−26]

$$\frac{F_{\text{elastic}}}{n} = \text{constant} + k_B T \frac{3}{2} \frac{1}{N_f l_f^2} R^2 \qquad (7)$$

We take the polymer as incompressible and obtain an expression for the layer thickness, R, as a function of the number of molecules, n, and area, A:

$$RA = nN_f v_f = \text{constant} \qquad (8)$$

Combining both equations yields

$$F_{\text{elastic}} = \text{constant} + k_B T \frac{3}{2} \frac{n^3 N_f v_f^2}{l_f^2} A^{-2} \qquad (9)$$

and the first derivative is given by

$$\frac{\partial F_{\text{elastic}}}{\partial A} = -3 k_B T \frac{N_f v_f^2}{l_f^2} \left(\frac{A}{n}\right)^{-3} \qquad (10)$$

(b) Semenov-Type Brush. In the second scenario, we assume that the chain ends are not fixed near the polymer/air interface, but we assume a distribution within the film that minimizes the free energy (see Figure 2b). As a consequence, the polymer chains are nonuniformly stretched. To obtain the conformational free energy of a single chain, one has to define a local stretching $\partial r/\partial N$, and replace $(R/N)R$ in eq 7 in the previous scenario by $f(\partial r/\partial N)\partial r$ (r, vertical distance from the head group; N, running number of the chain segment—at the head group $N = 1$, and at the free end $N = N$). It can be shown that, for an affine deformation, the above integral is proportional to $(R/N)R$. To obtain the corresponding expression for the complete brush, one has to take the weighted average over all possible conformations of the polymer chains. For Gaussian chains in the lamellar morphology of a phase-separated block copolymer melt, this problem has been solved by Semenov.[2,3]

Our system resembles very closely one half of the lamella investigated by Semenov. We assume that the results of Semenov can be applied to our asymmetric film, but, compared to his results, we only have half the number of polymers per unit surface of the film. Semenov gives an expression for the free energy of one polymer lamella per unit area:

$$\frac{F_{\text{elastic}}}{A}\Big|_{\text{lamella}} = \frac{4}{3} \frac{\pi^2}{32 a_f^2 N_f^2} R^3 \qquad (11)$$

In his expression, $k_B T$ and the volume of the link, v, are taken as unity. To have expressions in SI units, we substitute $F_{\text{elastic}}/k_B T$ for F_{elastic}, $a_f/(v_f)^{1/3}$ for a_f, $R/(v_f)^{1/3}$ for R, and $A/(v_f)^{2/3}$ for A. In addition, we substitute $l_f^2/6$ for a_f^2 and divide the expression by 2 in order to correct for the fact that our film represents only half the lamellar considered by Semenov:

$$\frac{F_{\text{elastic}}}{A} = \frac{\pi^2}{8} k_B T \frac{1}{l_f^2 N_f^2 v_f} R^3 \qquad (12)$$

We again apply eq 8 and take the first derivative of the elastic energy to obtain

$$\frac{\partial F_{\text{elastic}}}{\partial A} = -\frac{\pi^2}{4} k_B T \frac{N_f v_f^2}{l_f^2} \left(\frac{A}{n}\right)^{-3} \qquad (13)$$

This result is similar to the result obtained for the uniformly stretched brush in eq 10. Indeed, we expect the same power law in any scenario that involves affine deformation. The only difference is the numerical prefactor $\pi^2/4 \approx 2.47$, which is slightly lower than the prefactor of 3 in the former scenario. This result reflects the fact that, in the Semenov brush, the chains are allowed to assume thermodynamic equilibrium, while in the uniformly stretched brush they are fixed at thermodynamically unfavorable positions.

(c) Uniformly Stretched Brush, Langevin Approximation. If polymer chains are stretched to an end-to-end distance of more than one-third the fully extended length, the assumption of Gaussian chain statistics is no longer accurate. In this case, it is more accurate to use the inverse Langevin approximation. In an expansion of this approximation (truncated after the third term), one obtains[27]

$$\frac{F_{\text{elastic}}}{n k_B T} = \text{constant} + \frac{3}{2} \frac{1}{N_f l_f^2} R^2 + \frac{9}{20} \frac{1}{N_f^3 l_f^4} R^4 + \frac{99}{350} \frac{1}{N_f^5 l_f^6} R^6 \qquad (14)$$

If we apply the same procedures as have been used in the uniformly stretched Gaussian brush, we obtain the analogue of eq 10:

$$\frac{\partial F_{\text{elastic}}}{\partial A} = -N_f k_B T \left[3 \frac{v_f^2}{l_f^2} \left(\frac{A}{n}\right)^{-3} + \frac{9}{5} \frac{v_f^4}{l_f^4} \left(\frac{A}{n}\right)^{-5} + \frac{297}{175} \frac{v_f^6}{l_f^6} \left(\frac{A}{n}\right)^{-7} \right] \qquad (15)$$

For large areas per head group (low degree of stretching), this equation approaches, as expected, the Gaussian approximation.

We apply eqs 10, 13, and 15 to eq 2 and obtain

for Gaussian chains:

$$\Pi = \gamma^* + f\left(\frac{A}{n}, \text{ not } N_f\right) + k_B T N_f c \frac{v_f^2}{l_f^2} \left(\frac{A}{n}\right)^{-3} \qquad (16)$$

with

uniformly stretched brush $\quad c = 3$

Semenov brush $\quad c = \pi^2/4$

for non-Gaussian statistics:

$$\Pi = \gamma^* + f\left(\frac{A}{n}, \text{ not } N_f\right) + k_B T N_f \left\{ 3 \frac{v_f^2}{l_f^2} \left(\frac{A}{n}\right)^{-3} + \frac{9}{5} \frac{v_f^4}{l_f^4} \left(\frac{A}{n}\right)^{-5} + \frac{297}{175} \frac{v_f^6}{l_f^6} \left(\frac{A}{n}\right)^{-7} \right\} \qquad (17)$$

Two features of this description will be important in the following data treatment: (i) At a given area per head group (A/n), the "elastic part" of the surface pressure depends linearly on the chain length and (ii) for Gaussian chains, the elastic part of the surface pressure is proportional to the third power of the area per head group. To test the first prediction, one can plot the surface pressure data of different polymers but the same area per head group as a function of chain length. To test the second prediction, one might take the difference between the isotherms of polymers of different chain length and thus eliminate the first two terms in eq 17:

$$\Pi_1 - \Pi_2 = k_B T(N_{f1} - N_{f2}) c \frac{v_f^2}{l_f^2}\left(\frac{A}{n}\right)^{-3} \tag{18}$$

If we rescale the above equation by the cross-sectional area of the chain ($\alpha_f = v_f/l_f$), we obtain the dimensionless representation

$$\frac{\Delta\Pi}{\Delta N_f}\frac{\alpha_f}{k_B T} = c\left(\frac{A}{n}\frac{1}{\alpha_f}\right)^{-3} \tag{19}$$

Equation 20 predicts a straight line in the plot of $\log[(\Delta\Pi/\Delta N_f)(\alpha/k_B T)]$ vs $\log[(A/n)/(\alpha)]$, the intercept being given by the prefactor c. In this rescaled plot, all pairs of polymers will be represented by a single line, even if we compare chains of different flexibility.

$$\log\left(\frac{\Delta\Pi}{\Delta N}\frac{\alpha_f}{k_B T}\right) = \log c - 3\log\left(\frac{A}{n}\frac{1}{\alpha_f}\right) \tag{20}$$

Real Chains. Until now, we limited our considerations to freely jointed chains. A real chain, however, has bond angle and torsional restrictions. This chain is composed of N chemically identical repeat units, characterized by a length l and a volume v. It can be shown that, in this case, the mean square end-to-end distance is larger than Nl^2 but still proportional to N ($\langle r^2\rangle_0 > Nl^2$; $\langle r^2\rangle_0/N =$ constant). This sterically hindered chain, however, can be represented by an equivalent freely jointed chain, composed of N_f so-called Kuhn segments, which has the same undisturbed end-to-end distance, $\langle r^2\rangle_0 = N_f l_f^2$, and the same fully extended chain length, $Nl = N_f l_f$:

$$N_f = N\frac{l}{l_f} \tag{21}$$

$$l_f = \frac{\langle r^2\rangle_0}{Nl} \tag{22}$$

The conservation of the volume of the polymer chains leads to the additional condition

$$\frac{v_f}{l_f} = \frac{v}{l} \tag{23}$$

One can, therefore, either use experimental data on $\langle r^2\rangle_0/N$ and l to calculate the equivalent freely jointed chain or apply eqs 21−23 to eqs 17 and 20 to obtain for Gaussian brushes:

$$\frac{\Delta\Pi}{\Delta N}\frac{\alpha}{k_B T} = c\left(\frac{A}{n}\frac{1}{\alpha}\right)^{-3} \leftrightarrow \log\left(\frac{\Delta\Pi}{\Delta N}\frac{\alpha}{k_B T}\right) = \log c - 3\log\left(\frac{A}{n}\frac{1}{\alpha}\right) \tag{24}$$

for the inverse Langevin approximation:

$$\frac{\Delta\Pi}{\Delta N}\frac{\alpha}{k_B T} = \left[3\left(\frac{A}{n}\frac{1}{\alpha}\right)^{-3} + \frac{9}{5}\left(\frac{A}{n}\frac{1}{\alpha}\right)^{-5} + \frac{297}{175}\left(\frac{A}{n}\frac{1}{\alpha}\right)^{-7}\right] \tag{25}$$

with

$$\alpha = \frac{v}{\sqrt{\langle r^2\rangle_0/N}} \tag{26}$$

Experimental Section

Linear polyisoprenes with a *sec*-butyl group at one end and a sulfonate group at the other end have been prepared via anionic polymerization followed by reaction with diphenylethylene and propanesultone. The polymers were prepared in molecular masses between 10 and 50 kg mol^{-1}. The raw products, which generally had a narrow molecular weight but a degree of end group sulfonation between 20% and 90%, were purified via flash chromatography, followed by high-performance liquid chromatography (HPLC). The most likely counterion to the sulfonate group is Li^+, unless counterion exchange occurred, e.g., with the glass beakers or silica gel. The final products were pure within the detection limit of the analytical HPLC. The characterization of the polymers is summarized in Table 1. A general description of the synthesis is given in Appendix B. The polymers are colorless liquids of honey-like viscosity.

Trichloromethane (Aldrich, 99.99% pure) and ethanol (Aldrich, 99.99+% pure) were used as received. Water (resistivity 18.2×10^6 Ω cm^{-1}, total dissolved organic carbon <5 ppm) was purified with an ion exchange/filter system (Millipore).

Isotherms on the surface of pure water were recorded using a 20 cm × 46 cm rectangular Langmuir trough made of polytetrafluoroethylene, equipped with one compression barrier and a floating barrier for the detection of the surface pressure via the Langmuir method (FW2, Lauda GmbH, Lauda, Germany). The polymers were usually spread from chloroform solutions which contained 0.05 wt % of polymer and 10 wt % of ethanol. All isotherms were recorded at 20 °C. The number-average molecular weight was used to calculate the mean area per molecule of the polymers.

Silicon substrates were cleaned at 75 °C with a mixture of 5 parts water, 1 part ammonia solution (30 wt % in water), and 1 part hydrogen peroxide solution (35 wt % in water) and rinsed with purified water.

Monolayers were visualized using a Brewster Angle Microscope (BAM1) from NFT (Göttingen, Germany). The pictures were digitized, and the distortion of the images due to the observation at the Brewster angle was corrected with image-processing software. The images represent a 0.75 mm × 0.75 mm section of the trough area. The lateral resolution of the images is 4 μm.

Specular X-ray scattering was performed with a commercial $\theta/2\theta$ instrument (STOE & CIE GmbH, Darmstadt, Germany; $U = 40$ kV, $I = 50$ mA, $\lambda = 1.54$ Å (Cu Kα)). The divergence of the incident beam was 0.1°, and the 2θ resolution was 0.05°. Measurements typically lasted several hours and were performed at room temperature in air. The X-ray data were analyzed assuming a box model and using the software described in ref 28.

Results and Discussion

The following section is organized in four parts. We investigate (a) whether the polymers are surface active

Table 1. Characterization of the Polyisoprenes

	PI-SO_3-140	PI-SO_3-307	PI-SO_3-538	PI-SO_3-675	PI-SO_3-810
M_w/M_n	1.14	1.04	1.02	1.02	1.02
M_n (GPC) (H-terminated PI) (g/mol)	9638	20820	36540	45900	55020
no. of repeat units, N	140	307	538	675	810
no. of statistically equivalent chain segments (Kuhn segments), N_f	74	162	284	357	428
fully extended chain length, Nl (Å)	644	1412	2475	3105	3726
maximum film thickness, R_{max} (from eq 27) (Å)	180	250	400	470	510

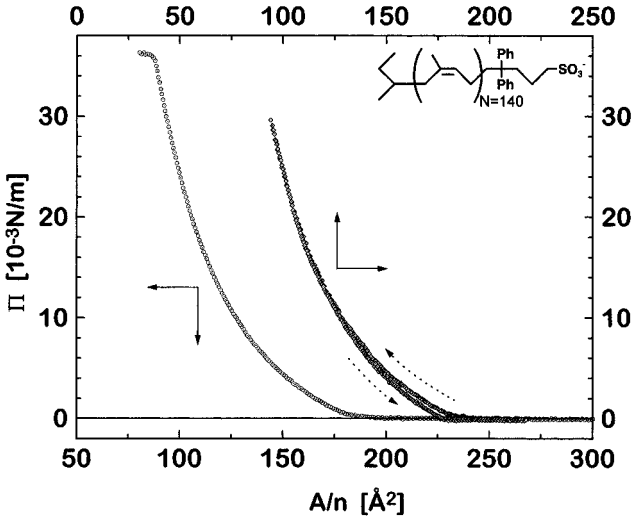

Figure 3. Isotherm and hysteresis measurement of PI-SO_3-140. For clarity, the data are horizontally shifted with respect to each other by 50 Å.

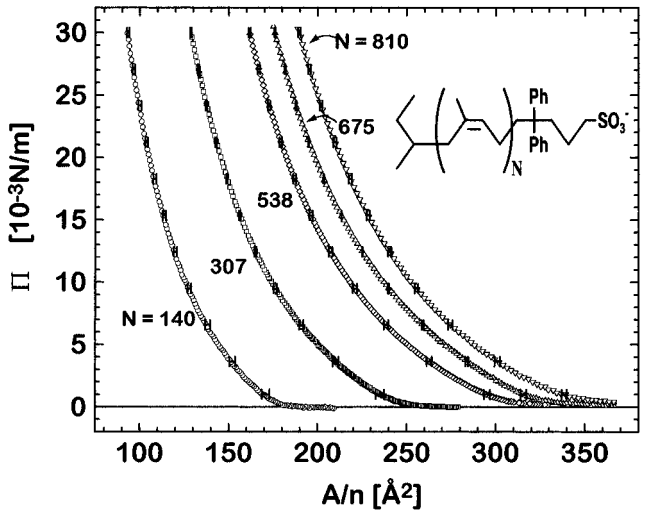

Figure 4. Isotherms of polyisoprenes of different chain length, N (averages of at least five measurements).

and isotherms can be recorded; (b) in which regime of the area per head group we have the uniform monolayer assumed in the theory; (c) whether the incompressibility condition given by eq 8 is valid; and finally (d) whether the isotherms agree with the theoretical description given above.

(a) Surface Activity/Isotherms. The polyisoprenes with sulfonate head groups can be spread onto the water surface from solutions in chloroform or mixtures of chloroform and ethanol, and isotherms of an expanded type can be recorded. The use of either ethanol or high dilution is necessary to obtain complete spreading. At a mass fraction of >0.15% of polymer in pure chloroform or at a content of <3 wt % of ethanol in the spreading solution, the isotherm shifts to lower areas per head group and depends on the spreading conditions. At the proper dilution or composition of the spreading solvent, however, the isotherms are independent of the spreading conditions. The corresponding polyisoprenes bearing no polar head groups do not form monolayers, when spread to the water surface, but retract into millimeter-size droplets and do not change the surface pressure once the spreading solvent is evaporated.

A drop of the solvent-free polymer with polar head groups, applied to the water surface, does not spread and does not give rise to a significant rise in surface pressure within 24 h.

The general features of an individual isotherm are shown in Figure 3, using polymer PI-SO_3-140. The isotherm is independent of compression speed and shows a collapse at surface pressures exceeding 35×10^{-3} N m^{-1}. At pressures below collapse, the isotherm is nearly free of hysteresis, the expansion cycle overlapping with the compression within the accuracy of the experiment. The isotherms of the five polymers investigated are shown in Figure 4 (averages of at least five different experiments). The isotherms significantly expand with increasing molecular weight. The collapse pressures of the polymers (not shown in Figure 4) are independent of the chain length.

It seems puzzling that the liquid polymers are surface active when spread from solution but do not spread on their own. We attribute this behavior to the fact that the ionic head groups form clusters in the nonpolar environment of the polymer.[29] These clusters are then sterically hindered against reaching the surface, and the spreading of a drop is very much slowed down. If the polymers are highly diluted in the polar chloroform, or if we add the even more polar ethanol to the spreading solution, these clusters dissociate. In the spreading process, the now isolated head groups can access the water surface and bind to it.

One might argue whether the monolayer or the polymer droplet is the thermodynamically stable state. The above theory, however, can be applied as well to a metastable film as long as the head groups do not leave the interface during the experiment and as long as the polymer chains are mobile and able to assume their equilibrium conformation. Because the isotherms are essentially free of hysteresis, these two conditions are fulfilled.

(b) Lateral Homogeneity. To test whether the polymer layer is laterally homogeneous, we investigated the polymer layer on the water surface using Brewster angle microscopy (BAM). The images presented in Figure 5 are taken in the order of decreasing area per head group. All pictures taken at areas per head group larger than the onset of the isotherm (Figure 5a–g) show a foamlike appearance. Between the onset of the isotherm and collapse, the images are essentially featureless (see Figure 5h), even if the analyzer of the BAM is rotated. After collapse (Figure 5i), a grainy structure appears.

The BAM pictures confirm the notion that, at areas larger than the onset of the isotherm, we do not have a continuous film. The dark areas most likely are "holes" in the monolayer which are compacted upon lateral

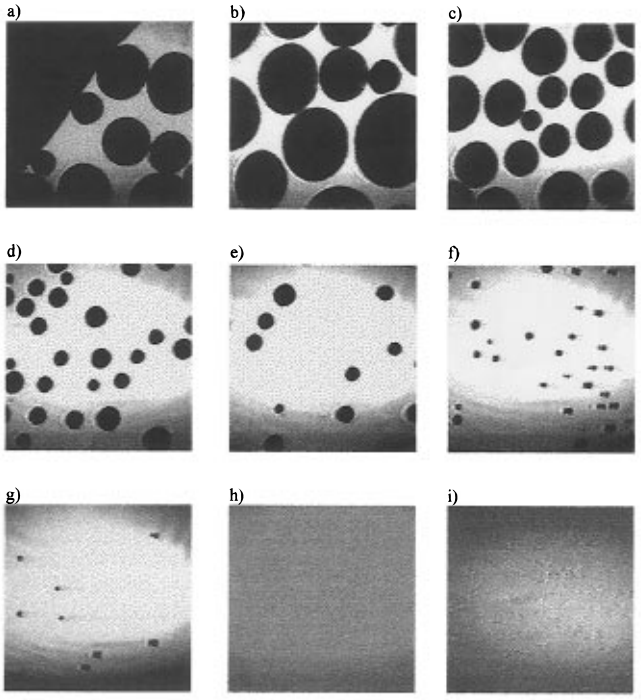

Figure 5. Monolayers of PI-SO_3-140 imaged with Brewster angle microscopy at various areas per head group. The pictures cover an area of approximately 0.75 mm × 0.75 mm. (a−g) A/n decreasing from initially 220 Å^2 in picture a to 185 Å^2 in picture g; (h) A/n = 130 Å^2; (i) A/n = 85 Å^2.

compression of the film and vanish at the onset of the isotherm. Comparable pictures have already been obtained in other polymeric systems.[30] The images also confirm the collapse point derived from the isotherm.

At least in the resolution limit of the BAM (4 μm), we cannot detect any structure in the film between the onset of the isotherm and the collapse. We therefore assume that we can apply, in this regime, the theory developed above.

(c) Film Thickness. One might take the incompressibility condition eq 8 for granted (see, e.g., refs 1, 2, and 4). This condition implies, however, that one can vary the film thickness of a monolayer of a single polymer simply by adjusting the area per head group:

$$R = Nv\left(\frac{A}{n}\right)^{-1} \tag{27}$$

This prediction might be of great value for the application of transferred films.

Therefore, we transferred films of PI-SO_3-140 and PI-SO_3-810 to hydrophilic silicon substrates at various surface pressures and measured the film thickness via X-ray reflectometry.

The transfer ratios were close to 1 in all cases. The q-dependent X-ray reflectivity of these films is depicted in Figure 6a,b. The reflectivities have been analyzed using a three-box model (Si/polyisoprene/air). The theoretical reflectivity has been fitted to the experimental data using five fit parameters (electron density of Si and of polyisoprene, film thickness of the polyisoprene layer, and the roughness of each of the interfaces between the boxes). The best fits to the data are represented in Figure 6a,b as continuous lines. The fit results are given in Table 2. In this analysis, we neglected the head groups and the native oxide layer on the silicon wafer. As a consequence, we obtain a relatively large error in the electron density of the

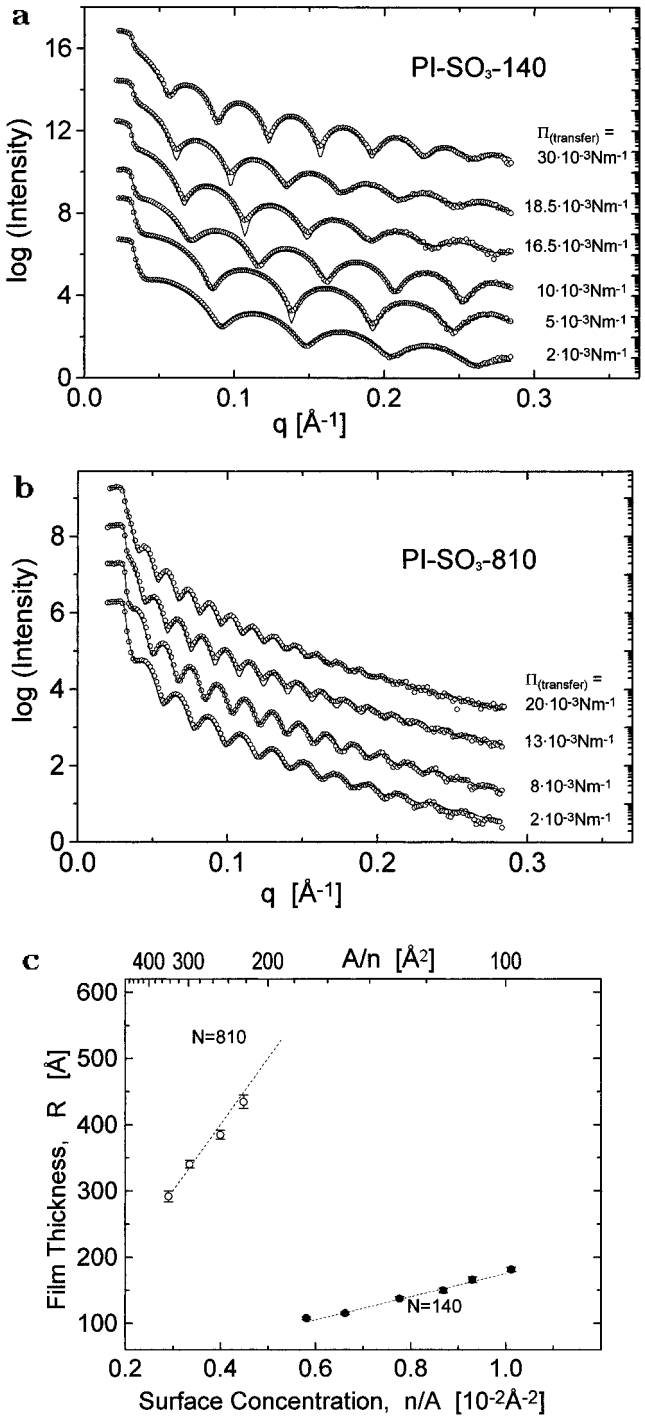

Figure 6. (a, b) q-dependent X-ray reflectivities of polymer monolayers transferred to silicon substrates at different surface pressure (polymer sample and pressure at transfer indicated in the diagram); q was calculated from the angle of reflection Θ and the wavelength of the X-rays λ according to $q = (4\pi/\lambda)\sin\Theta$. (c) Film thickness of monolayers of PI-SO_3-140 and PI-SO_3-810 that were transferred to silicon substrates at various surface concentrations. The points are experimental data, and the straight lines are the theoretical film thickness; calculated from bulk density and surface concentration according to eq 27.

polymer layer. The film thickness, however, has a standard deviation of ∼2%. In Figure 6c, the fitted film thickness is plotted versus the surface concentration of the head groups (inverse area per head group). The straight lines are calculated from eq 27 in the regime between the onset of the isotherm and collapse. Within the experimental error, the data agree with the theoretical predictions.

Table 2. Analysis of the X-ray Reflectivities and Fit Parameters of a Three-Box Model

polymer	film pressure at transfer, 10^{-3}N m^{-1}	film thickness, Å	δ(Si) = e$^-$-density/ ($\lambda^2 r_0/2\pi$) ($\times 10^{-6}$)	δ(PI) = e$^-$-density/ ($\lambda^2 r_0/2\pi$) ($\times 10^{-6}$)	roughness PI/air, Å	roughness PI/Si, Å
PI-SO_3-140	1	107.7 ± 2.2	7.47 ± 0.28	3.13 ± 0.58	4.0 ± 1.1	6.4 ± 2.3
PI-SO_3-140	5	115.1 ± 1.9	7.33 ± 0.09	3.04 ± 0.50	3.0 ± 2.2	6.5 ± 1.8
PI-SO_3-140	10	137.3 ± 2.6	6.89 ± 0.36	2.41 ± 1.02	3.0 ± 5.9	3.9 ± 2.1
PI-SO_3-140	16.6	149.7 ± 3.5	6.70 ± 0.07	2.87 ± 0.67	3.6 ± 2.1	9.0 ± 2.8
PI-SO_3-140	18.5	165.6 ± 2.6	7.34 ± 0.10	3.28 ± 0.62	3.7 ± 1.6	10.2 ± 3.6
PI-SO_3-140	30	181.4 ± 3.2	6.98 ± 0.18	2.60 ± 0.82	2.8 ± 3.3	7.9 ± 2.7
PI-SO_3-810	2	291.9 ± 8.0	7.25 ± 0.19	2.19 ± 0.45	9.5 ± 7.6	3.3 ± 1.4
PI-SO_3-810	8	340.5 ± 5.9	7.31 ± 0.01	2.29 ± 0.37	9.4 ± 5.2	4.2 ± 1.0
PI-SO_3-810	13	384.8 ± 6.8	7.29 ± 0.12	1.98 ± 0.49	8.0 ± 5.1	3.4 ± 1.3
PI-SO_3-810	20	434.6 ± 10	7.21 ± 0.03	1.93 ± 0.72	11.1 ± 13.2	3.3 ± 2.1
theor value			7.44[46]	3.27 (polyisoprene)[a] 3.33 (polystyrene)[46]		

[a] See Appendix C.

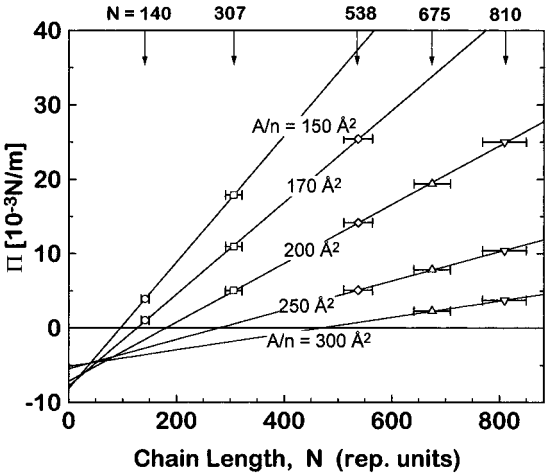

Figure 7. Surface pressure of PI-SO_3 film as a function of chain length at constant area per head group (same data as in Figure 4; for clarity, we show the data for only a limited number of areas per head group).

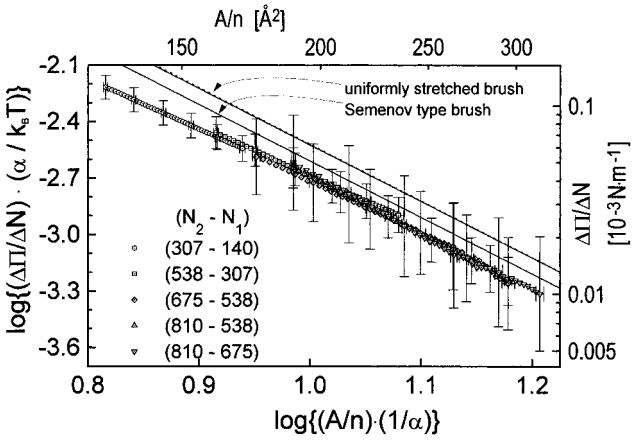

Figure 8. Double-logarithmic plot of pressure difference over chain length difference versus area per head group. The left and bottom axes are rescaled by the "cross-sectional area of a segment", $\alpha = v/(\langle r^2\rangle_0/N)^{1/2}$. Straight lines are the theoretical predictions from Gaussian statistics according to eq 24, and the dotted curve is the theoretical prediction based on the inverse Langevin approximation according to eq 25.

The maximum thickness of each film never exceeds one-third of the fully extended chain length (see Table 1). Therefore, we expect no significant deviations from Gaussian statistics due to an overstretching of the chains.

(d) Thermodynamic Analysis. In the preceding sections, we showed that the assumptions of the theory (equilibrium conformation of the chains, lateral homogeneity, and constant density of the film) are fulfilled by our system. We therefore apply the theoretical treatment proposed above.

In Figure 4, the surface pressure data for the polymers are presented as a function of area per head group, the chain length being the third parameter. To test the linear dependency of the surface pressure on the chain length, the data are replotted in Figure 7 as a function of chain length, the third parameter being now the area per head group. (For clarity, the data corresponding only to a limited number of areas per head group are represented.) The theoretically predicted linear dependency can only be tested in a regime of A/n where more than two isotherms can be measured. In this regime, between 170 and 250 Å^2, where we have three or four data points available, all these points fall onto a straight line, in accordance with the predictions.

To test the second theoretical prediction, we calculated the pressure differences between different isotherms and plotted them in a double-logarithmic representation against the area per head group according to eq 24 (see Figure 8). The straight lines in Figure 8 represent the theoretical predictions of eq 24 using the appropriate prefactors for the uniformly stretched and the Semenov brushes. The description of the uniformly stretched non-Gaussian brush (eq 25) is represented by the dashed curve.

We note that, in this double-logarithmic plot, the pressure differences between pairs of polymers actually can be represented by straight lines, the slope being close to the predicted value of −3. These individual lines, indeed, collapse into a single curve which, within the error of the experiment, can be represented by the theoretical description. The data seem to indicate that the description according to the Semenov theory is closer to reality than the uniformly stretched model.

Besides this general agreement between experiment and theory, we note that the experimental data in Figure 8 lie upon a slight bent curve with a slope between −2.7 and −3.1, rather than on a straight line, the deviation being most pronounced at lower areas per head group or for polymer chains shorter than 300 repeat units.

It seems likely that these data are based on polymers that are either too short or stretched too much to behave like Gaussian chains. We note, however, that chains of more than $N_f = 50$ segments can be considered long enough for Gaussian statistics[31] and that the extension of the chains in our system is too weak to cause significant deviation from Gaussian statistics. The latter fact is reflected in the insignificant difference between the Gaussian and the inverse Langevin approximation in Figure 8. Regardless of the details of

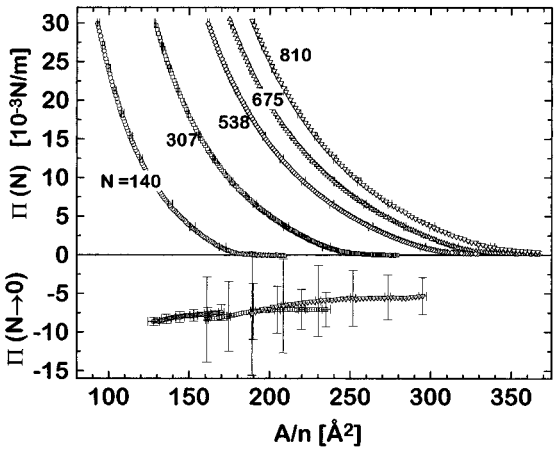

Figure 9. Linear extrapolation of the surface pressure down to zero chain length (bottom part) compared to the experimental isotherms.

the model used in the analysis, however, any affine deformation of the polymer film should give rise to a straight line with slope −3 in the double-logarithmic representation of Figure 8. Therefore, deviations from that slope might indicate deviations from affine deformation.

Until now, we have been interested exclusively in the "elastic" component of the surface pressure, which is due to the statistics of the polymer chains. To estimate the relative importance of this contribution, we linearly extrapolate the surface pressure data in Figure 7 down to zero chain length and obtain the first two terms of eq 6:

$$\Pi_{(N\to 0)} = \gamma^* + f\left(\frac{A}{n}, \text{ not } N\right) \tag{28}$$

The extrapolated data are shown in Figure 9 in comparison to the original isotherms. We extrapolate to values of N far away from our data. Hence, the data are rather inaccurate and have a large error. The pressures extrapolated to zero chain length are in the negative pressure range. This can be expected on the basis of the fact that $\gamma^* = \gamma_{wa} - (\gamma_{pa} + \gamma^\circ_{wp}) = -13 \times 10^{-3}$ N m^{-1} is negative (see Appendix C). Besides this effect of shifting the isotherm downward, $\Pi_{(N\to 0)}$ only weakly depends on the area per head group. Hence, the shape of the isotherm is dominated by the chain statistics of the polymers.

We expect $f(A/n)$ to increase with increasing surface concentration; in a first approximation, we expect $f(A/n) = 2k_BT(A/n)^{-1}$.[32,33] In contrast, $\Pi_{(N\to 0)}$ decreases with decreasing A/n. This effect is most noticeable in the regime of A/n where the data deviate most from the theory in Figure 8. The two deviations might, therefore, be correlated, and the dependency of $\Pi_{(N\to 0)}$ on A/n might reflect an inaccuracy of the theory which is amplified by the extrapolation procedure.

Conclusion

It has been shown that hydrophobic polymers with a single ionic head group and a chain length of up to 3200 atoms can form stable monolayers on the water surface and that these films can be transferred to solid substrates. We can regard these monolayers as an incompressible polymer melt tethered to a planar interface. Therefore, they are suitable for the preparation of thin polymer layers of controlled thickness and as model systems for studying the properties of dense solvent free brushes.

To our knowledge, this is the first description of isotherms that are dominated by the elastic deformation of polymer coils and can be described using Gaussian chain statistics. The best description is given by the nonuniformly stretched brush (Semenov theory). We observe deviations between theory and experiment which cannot be explained on the basis of deviations from Gaussian statistics due to overstretching or an insufficient number of repeat units.

Acknowledgment. We thank S. Förster for vital discussions concerning the anionic polymerization and the preparation of preliminary polymers; Profs. M. Antonietti and H. Möhwald for stimulating discussions; G. Czichocki, A. Martins, and P. Müller for analytical and preparative HPLC; G. Rother and J. Moskalenko for the determination of molecular weight via size exclusion chromatography; Ch. Merkl for help in the X-ray reflectivity studies, and V. Melzer and G. Weidemann for their help in the BAM studies. We thank the Deutsche Forschungsgemeinschaft and the Max Planck Society for financial support.

Appendix A: van der Waals Interaction between Air and Water through the Polymer Film

The free energy of van der Waals interaction between two planar surfaces of the media A and B separated by a thin layer of material C is given by[34]

$$\frac{F}{A} = -\frac{H}{12\pi R^2} \tag{A1}$$

where H is the Hamaker constant. We use the incompressibility condition,

$$RA = nNv \tag{A2}$$

and obtain

$$F = -\frac{HA^3}{12\pi(nNv)^2} \tag{A3}$$

We take the first derivative and apply eq A2 once again:

$$\frac{\partial F}{\partial A} = -\frac{HA^2}{4\pi(nNv)^2} \tag{A4}$$

$$\frac{\partial F}{\partial A} = -\frac{H}{4\pi R^2} \tag{A5}$$

This contribution to the surface pressure will be most prominent for thinner films. We therefore expect the strongest contribution for the shortest polymer at the onset of the isotherm ($R \approx 10^{-8}$ m). If we assume a Hamaker constant of 10^{-20} N·m,[35] we can expect a contribution of less than 0.1×10^{-3} N m^{-1} (the lower limit of accuracy of our measurement). In all other cases the contributions will be even lower. Therefore, we neglect the van der Waals interaction between air and water.

Appendix B: Synthesis of the Polyisoprenes

Polyisoprene was synthesized via living anionic polymerization using a high-vacuum nitrogen distribution line and a reactor similar to that described in ref 36.

Caution: The sodium−potassium alloy and the lithium−organic compounds are extremely flammable and might ignite spontaneously; propanesultone is a carcinogenic substance.

THF (Aldrich, 99+% pure), methylcyclohexane (Aldrich, 99% pure), and isoprene (Fluka, 98% pure) were purified according to ref 36. Nitrogen (Messer Griessheim, 99.999+% pure) was passed through a column filled with silica-supported phosphorus(V) oxide (Sicapent, Merck) and through tetraethylene glycol dimethyl ether (Aldrich, 99% pure) which contained ∼1 g of naphthalene (Aldrich, 99% pure) and sodium−potassium alloy. 1,1-Diphenylethylene (Aldrich, 97% pure) and 1,3-propanesultone (Aldrich, 99+% pure) were stirred with 5 vol % *n*-butyllithium (Aldrich, 2.0 mol/L solution in cyclohexane) and vacuum distilled prior to use. *sec*-Butyllithium (Aldrich, 1.3 mol/L solution in cyclohexane/heptane (90:10)), methanol (Roth, 99% pure) and 2-propanol (Roth, 99% pure) were used as received.

Polymerization Procedure. A mixture of 50 mL of isoprene and 300 mL of methylcyclohexane was equilibrated at 40 °C. While stirring, the calculated amount of the initiator *sec*-butyllithium was added rapidly through a rubber septum using a gas-tight syringe (Hamilton). The color of the solution changed slightly to yellow. After 60−90 min (depending on the molar mass of the polymer[37]), the solution was cooled to −90 °C, and 200 mL of THF was condensed into the reactor. Then a 2-fold excess of a 10 vol % solution of 1,1-diphenylethylene in THF was added dropwise with a gas-tight syringe. The color of the solution changed immediately to dark red. After 30 min of stirring, a 1.3-fold excess (with respect to the initiator) of a 10 vol % solution of 1,3-propanesultone in THF was added dropwise with a gas-tight syringe. The solution was then stirred at −90 °C until the color completely disappeared (∼60 min). After warming to room temperature, the reaction mixture was precipitated into 2 L of a 2:1 mixture of methanol and 2-propanol.

Chromatographic Purification and Characterization of the Polymer. In accordance with data on polystyrene,[38] the head group sulfonation of polyisoprene via 1,3-propanesultone yielded sulfonyl-terminated main product as well as hydrogen-terminated side product. This side product can be separated completely by flash chromatography (for $M_n > 20\,000$ g mol^{-1}) or preparative HPLC.[39] The molar mass was determined by GPC (calibrated with polyisoprene standards) using the hydrogen-terminated side product. According to NMR data, the polymer is composed of 71% 1,4-*cis*-, 22% 1,4-*trans*, and 7% 3,4-isoprenyl subunits.

Appendix C: Calculation of the Molecular Parameters

The parameters used in the data treatment were calculated as follows. The segment length, l, was calculated from molecular models built with the simulation program Hyperchem.[40] Because our polymer is actually a copolymer of 71% 1,4-*cis* units, 22% 1,4-*trans* units, and 7% 3,4 units, we estimated the lengths of these units separately (l(*cis*) = 4.6 Å, l(*trans*) = 5.0 Å, and l(3,4) = 2.7 Å) and calculated the mean length of a repeat unit as the weighted average l = 4.6 Å.

$(\langle r^2\rangle_0/N)^{1/2}$ was calculated from the constant $(\langle r^2\rangle_0/M)^{1/2} = 7.66 \times 10^{-11}$ m g$^{-1/2}$ mol$^{1/2}$ [41] (M = molecular mass of the polymer) and the mass of the repeat unit, m = 68 g/mol, according to $(\langle r^2\rangle_0/N)^{1/2} = (\langle r^2\rangle_0/M)^{1/2} m^{1/2} = 6.32$ Å. We note, however, that the data given in the literature on $\langle r^2\rangle_0/M$ scatter by approximately 10%.

l_f was calculated according to $l_f = (\langle r^2\rangle_0/N)/l = 8.7$ Å. N_f was calculated according to $N_f = N(l/l_f) = 0.53N$.

v was derived from the density of the polymer, ρ = 913 kg m^{-3},[42] and the molar mass of the repeat unit, m = 68 g/mol, according to $v = m/(N_A\rho) = 123.7$ Å^3.

$\gamma^* = \gamma_{wa} - (\gamma_{pa} + \gamma^\circ_{wp}) = -13 \times 10^{-3}$N m^{-1} can be calculated from the surface tension of clean water, $\gamma_{wa} = 72.9 \times 10^{-3}$N m^{-1},[43] the surface tension of the polymer, $\gamma_{pa} = 31 \times 10^{-3}$N m^{-1},[44] and the interfacial tension of the polymer water interface, γ°_{wp}. We calculated $\gamma^\circ_{wp} = 54.7 \times 10^{-3}$N m^{-1} from the contact angle between polymer and water, $\Theta = 109°$,[44] according to the Young equation,[45] $\gamma_{pa} - \gamma_{wp} = \gamma_{wa} \cos\Theta$.

q was calculated from the angle of reflection Θ and the wavelength of the X-rays λ according to $q = (4\pi/\lambda) \sin\Theta$.

δ(polyisoprene) $= 3.27 \times 10^{-6}$ was calculated from the electron density ρ_e, the wavelength λ of the X-ray beam, and the classical electron radius $r_0 = 2.82 \times 10^{-15}$ m according to $\delta = \rho_e/(\lambda^2 r_0/2\pi)$,[46] while $\rho_e = 0.307$ Å^{-3} was calculated from the density of polyisoprene, ρ, the molar mass of the repeat unit, m, and the number of electrons per repeat unit, z = 38, according to $\rho_e = z\rho(N_A/m)$.

Supporting Information Available: Isotherms of the investigated polymers (5 pages). Ordering information is given on any current masthead page.

References and Notes

(1) Helfand, E. *Macromolecules* **1975**, *8*, 552.
(2) Semenov, A. N. *Sov. Phys. JETP* **1985**, *61*, 733.
(3) Semenov, A. N. *Macromolecules* **1993**, *26*, 6617.
(4) Ohta, T.; Kawasaki, K. *Macromolecules* **1986**, *19*, 2621.
(5) Millner, S. T. *J. Polym. Sci. B* **1994**, *32*, 2743.
(6) Review article: Bates, F. S.; Fredrickson, G. H. *Annu. Rev. Phys. Chem.* **1990**, *41*, 525.
(7) vandePas, J. C.; Olsthoorn, Th. M.; Schepers, F. J.; deVries, C. H. E.; Buytenhek, C. J. *Colloid Surf.* **1994**, *85*, 221.
(8) Hristova, K.; Needham, D. *Macromolecules* **1995**, *28*, 991.
(9) For an introduction to the characterization and transfer of insoluble films, see: Gaines, G. L., Jr. *Insoluble Monolayers at Liquid-Gas Interfaces*; Interscience: New York, 1966. Roberts, G. *Langmuir−Blodgett Films*; Plenum Press: New York, 1990. Ulman, A. *An Introduction to Ultrathin Organic Films*; Academic Press: San Diego, CA, 1991.
(10) Alexander, S. *J. Phys.* **1977**, *38*, 983.
(11) deGennes, P. G. *Macromolecules* **1980**, *13*, 1069.
(12) Milner, S. T.; Witten, T. A.; Cates, M. E. *Macromolecules* **1988**, *21*, 2610.
(13) Venema, P.; Odijik, T. *J. Phys. Chem.* **1992**, *96*, 3922.
(14) Wijmans, C. M.; Scheutjens, J. M. H. M.; Zhulina, E. B. *Macromolecules* **1992**, *25*, 2657.
(15) Review article: Halperin, A.; Tirrell, M.; Lodge, T. P. *Adv. Polym. Sci.* **1992**, *100*, 31.
(16) Kent, M. S.; Lee, L.-T.; Farnoux, B.; Rondelez, F. *Macromolecules* **1992**, *25*, 6231.
(17) Milner, S. T. *Europhys. Lett.* **1988**, *7*, 659.
(18) Granick, S.; Herz, J. *Macromolecules* **1985**, *18*, 460.
(19) Kim, M. W.; Chung, T. C. *J. Colloid Interface Sci.* **1988**, *124*, 365.
(20) Christie, P.; Petty, M. C.; Roberts, G. G. *Thin Solid Films* **1985**, *134*, 75.
(21) Goedel, W. A.; Xu, C.; Frank, C. W. *Langmuir* **1993**, *9*, 1184.
(22) Lenk, T. J.; Lee, D. H. T.; Koberstein, J. T. *Langmuir* **1994**, *10*, 1857.
(23) Mirley, C. L.; Koberstein, J. T. *Langmuir* **1995**, *11*, 1049.
(24) Treloar, L. R. G. *The Physics of Rubber Elasticity*; Clarendon Press: Oxford, 1975; pp 56/57.
(25) deGennes, P. G. *Scaling Concepts in Polymer Physics*; Cornell University Press: Ithaca & London, 1979; p 31.
(26) Mark, J. E.; Erman, B. *Rubberlike Elasticity a Molecular Primer*; Wiley & Sons: New York, Chichester, Singapore, 1988; p 30.

(27) Reference 24, pp 104−106.
(28) Asmussen, A.; Riegler, H. *J. Chem. Phys.* **1996**, *104*, 8159.
(29) Davidson, N. S.; Fetters, L. J.; Funk, W. G.; Graessley, W. W.; Hadjichristidis, N. *Macromolecules* **1988**, *21*, 112.
(30) Mann, E. K.; Henon, S.; Langevin, D.; Meunier, J. *J. Phys. II Fr.* **1992**, *2*, 1683.
(31) Reference 24, pp 109−111.
(32) Davies, J. T.; Rideal, E. K. *Interfacial Phenomena*; Academic Press: New York and London, 1961; pp 231−234.
(33) Eriksson, J. C.; Ljunggren, S. *Colloid Surf.* **1989**, *38*, 179.
(34) Israelachvili, J. *Intermolecular & Surface Forces*; 2nd ed.; Academic Press: London, 1991, p 177.
(35) See, for comparison, ref 34, p 191.
(36) Ndoni, S.; Papadakis, C. M.; Bates, F. S.; Almdal, K. *Rev. Sci. Instrum.* **1995**, *2*, 66.
(37) Young, R. N.; Quirk, R. P.; Fetters, L. J. *Adv. Polym. Sci.* **1984**, *56*, 1−90.
(38) Möller, M.; Mühleisen, E.; Omeis, J. In *Physical Networks—Polymers and Gels*; Burchard, W., Ross-Murphy, S. B., Eds.; Elsevier Applied Science: London, 1990; pp 45−64. Mühleisen, E. Ph.D. Thesis, Freiburg i. Br., Germany, 1989.
(39) Czichocki, G.; Heger, R.; Goedel, W. A.; Much, H. Submitted to *J. Chromatogr.*
(40) *Hyperchem*; Hypercube Inc., Waterloo, Ontario, Canada.
(41) Brandrup, J., Immergut, E., Eds. *Polymer Handbook*, 3rd ed.; Wiley: New York, 1989; p VII/33. Prud'homme, J.; Roovers, J. E. L.; Bywater, S. *Eur. Polym. J.* **1972**, *8*, 901.
(42) Polymer Handbook V/7: Wood, L. A. *Rubber Chem. Technol.* **1939**, *12*, 130.
(43) Gaonkar, A. G.; Neumann, R. D. *Colloids Surf.* **1987**, *27*, 1.
(44) Lee, L. H. *J. Polym. Sci., A-2* **1967**, *5*, 1103.
(45) Hiemenez, P. C. *Principles of Colloid & Surface Chemistry*, 2nd ed.; Marcel Dekker: New York & Basel, 1986; p 308. Brezesinski, G.; Mögel, H. J. *Grenzflächen & Kolloide*; Spektrum Akademischer Verlag: Heidelberg/Berlin/Oxford, 1993; p 56.
(46) Russel, T. P. *Mater. Sci. Rep., Rev. J.* **1990**, *5* (415), 175.

MA9608378